

Photochemical Reactions of Aromatic Compounds. Part 44.¹ Mechanisms for Direct Photoamination of Arenes with Ammonia and Amines in the Presence of *m*-Dicyanobenzene

Masahide Yasuda,* Yoriaki Matsuzaki, and Kensuke Shima

Department of Industrial Chemistry, Faculty of Engineering, Miyazaki University, Kumano, Miyazaki 889-21, Japan

Chyongjin Pac*

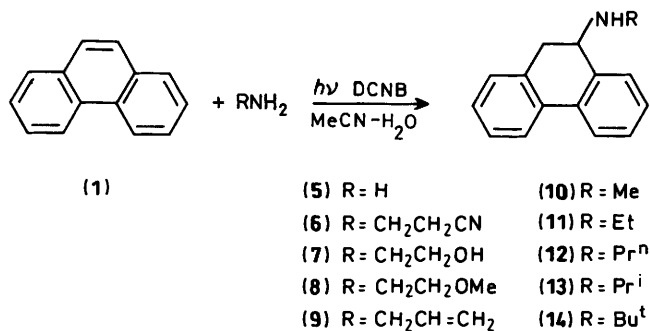
Department of Chemical Process Engineering, Faculty of Engineering, Osaka University, Yamadaoka, Suita, Osaka 565, Japan

Mechanistic details of the efficient photoamination of arenes (ArH) with ammonia or aliphatic primary amines (RNH₂) in the presence of *m*-dicyanobenzene (DCNB) in 9:1 acetonitrile–water have been analysed by kinetics. The initiation process of the photoamination is electron transfer from excited singlet ArH to DCNB to generate the cation radical of ArH (ArH^{•+}), to which RNH₂ undergoes nucleophilic addition. The rate constant (k_N) for the nucleophilic addition to the phenanthrene cation radical depends on R, varying from 3×10^7 dm³ mol⁻¹ s⁻¹ for NH₃ to 8.9×10^8 dm³ mol⁻¹ s⁻¹ for Bu^tNH₂. A plot of log k_N versus the Taft σ^* parameter is linear with a slope of -2.1, demonstrating a substantial positive charge on RNH₂ in the transition state in line with the proposed mechanism. Photoamination with Me₂NH is very inefficient for naphthalene, 2-methoxynaphthalene, and phenanthrene, and is attributed to electron exchange between ArH^{•+} and Me₂NH being competitive with nucleophilic addition. Anthracene is efficiently photoaminated with Me₂NH but inefficiently with Et₂NH. Efficient photoamination requires that the observed oxidation potential of the amines is more positive by 0.3–0.4 eV than that of ArH.

As part of our investigation on the synthetic applications of photoelectron transfer,^{1–6} we have reported that a variety of arenes (ArH) are efficiently aminated with ammonia and primary amines (RNH₂) upon irradiation in the presence of an electron acceptor, thus providing an excellent tool for the direct introduction of amino groups into unactivated arenes. In previous papers on the synthetic aspects of the photoamination,^{1,6} we proposed a working hypothesis that RNH₂ adds to the cation radical of ArH generated by electron transfer in the excited singlet state. In general, however, reactions of cation radicals with nucleophiles may arise from electron exchange⁷ or from π -complex formation⁸ followed by chemical processes, though nucleophilic addition is most probable for the photoamination with RNH₂. In this regard, it should be noted that photoamination with secondary amines (R₂NH) reveals interesting features different from that with RNH₂. In order to explore the general mechanistic aspects of the photoamination, we have extensively investigated the kinetics of photoamination of phenanthrene with a variety of primary amines as well as details of the photoreactions of some selected arenes with secondary amines.

Results

Kinetic Results for the Photoamination of Phenanthrene with RNH₂.—The photoamination of phenanthrene (1) with a variety of amines RNH₂ in the presence of *m*-dicyanobenzene (DCNB) in 9:1 acetonitrile–water gave the phenanthrene derivatives (5)–(14) in >80% yields along with >90% recovery of DCNB (Scheme 1). Figures 1 and 2 show double-reciprocal plots of quantum yield (ϕ) for the formation of the aminated products versus the concentration of DCNB and versus the concentration of RNH₂, respectively, as typical examples. Such linear plots were also obtained from the other amines. The slopes and intercepts of the plots are listed in Table 1.



Scheme 1.

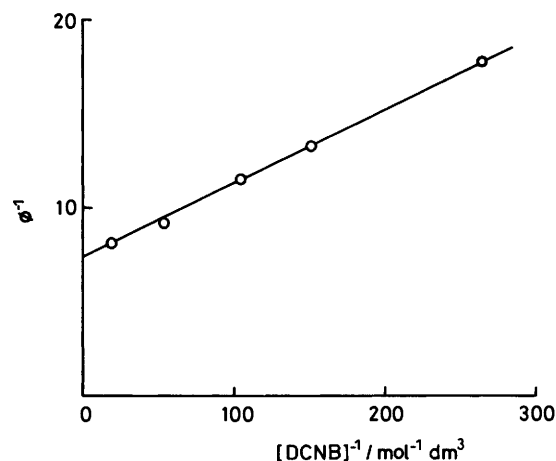


Figure 1. A double-reciprocal plot of ϕ versus $[\text{DCNB}]$ for the photoamination of (1) with PrⁿNH₂; [(1)] 0.05 mol dm⁻³ and [PrⁿNH₂] 0.25 mol dm⁻³; 313 nm irradiation

Table 1. Kinetic data from double-reciprocal plots of quantum yields versus concentration of DCNB or RNH₂ for photoamination of phenanthrene (1)^a

Reactant ^b	Intercept (I)	Slope (S)	r ^c
DCNB	7.4	0.039	0.999
NH ₃	2.2	2.4	0.984
NCCH ₂ CH ₂ NH ₂	2.2	0.66	0.984
HOCH ₂ CH ₂ NH ₂	2.8	1.45	0.996
MeOCH ₂ CH ₂ NH ₂	2.4	1.09	0.996
CH ₂ =CHCH ₂ NH ₂	7.1	1.43	0.999
MeNH ₂	4.7	0.74	0.998
EtNH ₂	6.5	0.50	0.998
Pr ⁿ NH ₂	6.2	0.47	0.994
Pr ⁱ NH ₂	6.5	0.25	0.978
Bu ⁿ NH ₂	7.3	0.26	0.984

^a For 9:1 (v/v) acetonitrile–water solutions containing (1) [0.05 mol dm⁻³], DCNB, and RNH₂ irradiated at 313 nm. ^b Reactants for concentration change. For a plot of ϕ^{-1} versus [DCNB]⁻¹, [PrⁿNH₂] 0.25 mol dm⁻³, whereas [DCNB] 0.05 mol dm⁻³ for plots of ϕ^{-1} versus [RNH₂]⁻¹. ^c Standard correlation factors of the plots.

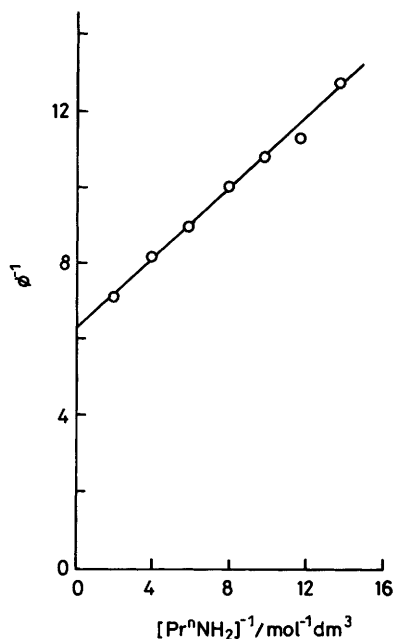


Figure 2. A double-reciprocal plot of ϕ versus [PrⁿNH₂] for the photoamination of (1); [(1)] 0.05 mol dm⁻³ and [DCNB] 0.05 mol dm⁻³; 313 nm irradiation

The photoamination of (1) with RNH₂ was efficiently quenched by either *p*-dimethoxybenzene or 1,3,5-trimethoxybenzene (Q) under the conditions where fluorescence quenching by Q is negligible. Kinetic analyses for quenching were carried out for photoamination with PrⁿNH₂. Quantum yields in the presence of a variable [Q] were determined at a given concentration of the amine, giving a linear Stern–Volmer plot (Figure 3). Such linear plots were obtained at several points of concentration of the amines. The results are listed in Table 2 including the slopes of the Stern–Volmer plots (K_{SV}).

Photoreactions of Some Arenes with Secondary Amines.—Table 3 shows chemical yields of the products isolated and the limiting quantum yields (ϕ^∞) for the formation of the photoaminated products from the photoreactions of (1),

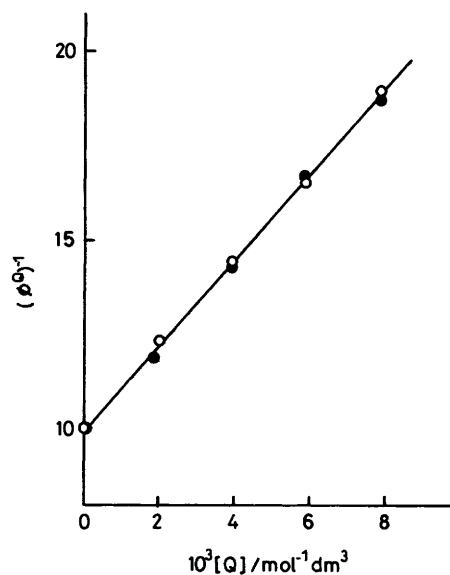


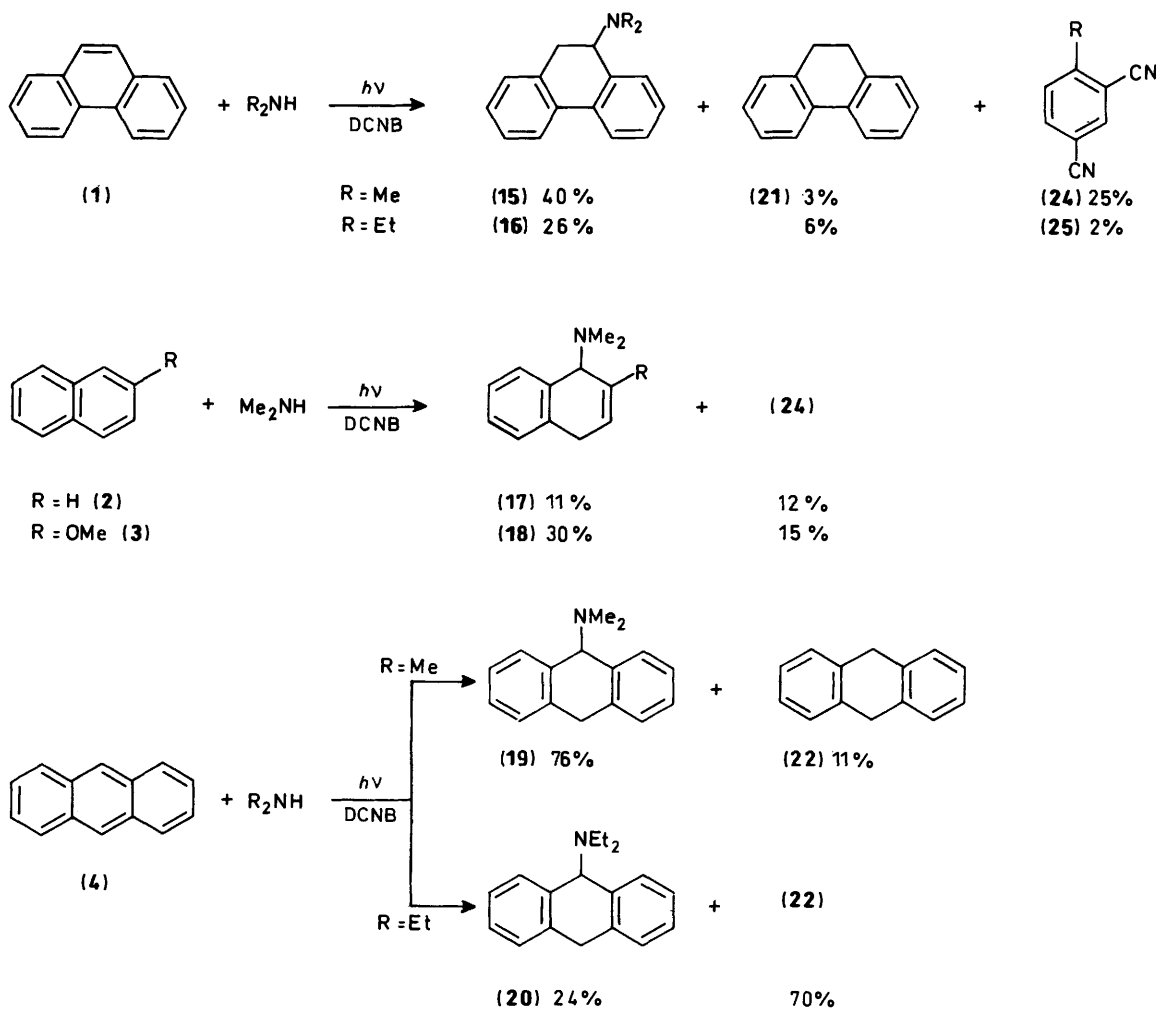
Figure 3. Stern–Volmer plots of $(\phi^0)^{-1}$ versus [Q] for quenching of photoamination of (1) (0.05 mol dm⁻³) with PrⁿNH₂ (0.125 mol dm⁻³) by *p*-dimethoxybenzene (○) and by 1,3,5-trimethoxybenzene (●); [DCNB] 0.05 mol dm⁻³; 313 nm irradiation

naphthalene (2), 2-methoxynaphthalene (3), and anthracene (4) with R₂NH (R = Me and Et). The photoreactions of (1)–(3) with R₂NH are complex, giving the aminated products only in poor yield. Moreover, DCNB was substantially consumed to give intractable materials, from which 1-alkyl-2,4-dicyanobenzenes (24) and (25) were isolated. On the other hand, anthracene (4) was efficiently photoaminated with Me₂NH to give the product (19) in 76% yield; the quantum yield for the disappearance of (4) is 0.32. Interestingly, however, the photoreaction of (4) with Et₂NH mainly gave 9,10-dihydroanthracene (22) in 70% yield along with the formation of the aminated product (20) in 24% yield, while the recovery of DCNB was quantitative (Scheme 2).

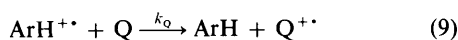
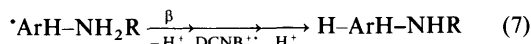
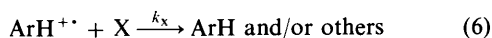
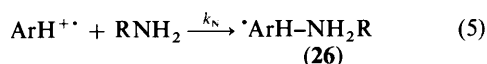
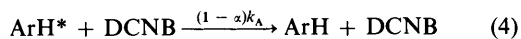
Discussion

Kinetic Analysis and Mechanism of Photoamination of (1) with RNH₂.—As discussed earlier,^{1,6} this photoamination is initiated by electron transfer from the excited singlet state of (1) to DCNB which gives the cation radical of (1) and the anion radical of DCNB, since the fluorescence of (1) is quenched by DCNB at a diffusion-controlled limit but not at all by RNH₂ (Table 4). With regard to the mechanistic discussion, it should be noted that the oxidation potential of RNH₂ is much more positive than that of (1), too high for electron exchange between (1)⁺⁺ and RNH₂ to occur. In fact, we were unable to detect any product that would be formed from RNH₂⁺, e.g. EtNH–NH₂Et, MeCH(NH₂)CH(NH₂)Me, and/or MeCHO from EtNH₂. Moreover, the photoamination was very clean, and DCNB was quantitatively recovered. For kinetic analysis, therefore, we assume equations (1)–(10) involving the nucleophilic addition of RNH₂ to (1)⁺⁺ as a key pathway.





Scheme 2.

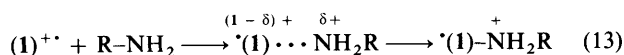


$$\varphi^{-1} = \frac{1}{\alpha\beta} \left(1 + \frac{1}{k_A\tau[\text{A}]} \right) \left(1 + \frac{k_X}{k_N[\text{RNH}_2]} \right) \quad (11)$$

$$\varphi^{-1} = \frac{1}{\alpha\beta} \left(1 + \frac{k_X}{k_N[\text{RNH}_2]} \right) \quad (12)$$

In the absence of a quencher (Q), steady-state analysis gives equation (11) where α and β denote the fractions for formation of free $\text{ArH}^{+\cdot}$ and for the formation of the aminated products (5)–(14) from adduct cation radical (26) respectively. The intercept-to-slope ratio of the plot in Figure 1 ($191 \text{ dm}^3 \text{ mol}^{-1}$) shows a satisfactory agreement with the Stern–Volmer constant for quenching of the fluorescence of (1) by DCNB ($242 \text{ dm}^3 \text{ mol}^{-1}$), clearly demonstrating that $^1\text{ArH}^*$ is responsible for the initiation of the photoamination. Therefore, equation (11) can be reduced to (12), since $k_A\tau[\text{DCNB}] \gg 1$ at 0.05 mol dm^{-3} DCNB where most kinetic experiments were carried out.

According to equation (12), the intercept of a double-reciprocal plot of φ versus $[\text{RNH}_2]$ in Figure 2 equals $1/\alpha\beta$ and then k_N/k_X can be obtained as the intercept:slope ratio for a given RNH_2 (I/S)_R. Table 5 lists the values of (I/S)_R and $\log (I/S)_R$ for each RNH_2 . It is reasonable to assume that relative values of (I/S)_R represent relative k_N since k_X of (1)^{+\cdot} can be considered to be independent of RNH_2 . In other words, $(I/S)_R/(I/S)_{\text{Me}} \approx k_N^R/k_N^{\text{Me}}$. Figure 4 shows a linear correlation of $\log [(I/S)_R/(I/S)_{\text{Me}}]$ with Taft σ^* , which gives a relatively large negative slope (-2.1) similar to that obtained for $\text{p}K_a$ of RNH_2 (-3.14).⁹ Therefore, a substantial positive charge should be populated on the nitrogen atom of RNH_2 in the transition state of the reaction which seems to be rather close to the product side along the reaction co-ordinate of equation (13), i.e.



$0 \ll \delta < 1$, thus supporting the suggested mechanism involving nucleophilic addition of RNH_2 to $\text{ArH}^{+\cdot}$. Possible participation

Table 2. Quenching of photoamination of (1) with Pr^nNH_2 by *p*-di- or 1,3,5-tri-methoxybenzene (Q)^a

$10^3[\text{Q}]$ mol dm ⁻³	$[\text{Pr}^n\text{NH}_2]$ mol dm ⁻³	$(\varphi^0)^{-1}$ ^b				
		0.1	0.125	0.167	0.25	0.50
0		10.8	10.1 (10.1)	8.9	8.2	7.1
2		13.9	12.4 (11.8)	10.3	9.5	7.9
4		17.4	14.5 (14.2)	12.1	10.5	8.5
6		19.9	16.5 (16.9)	14.5	11.8	9.4
8		24.0	19.1 (18.6)	16.4	13.4	9.8
$10^{-2}K_{\text{SV}}^c/\text{dm}^3 \text{ mol}^{-1}$		16.1	11.1 (11.0)	9.6	6.3	3.5

^a For 9:1 acetonitrile–water solution; $[(1)]$ 0.05 and $[\text{DCNB}]$ 0.05 mol dm⁻³; 313 nm irradiation. ^b Values in parentheses are $(\varphi^0)^{-1}$ for quenching by 1,3,5-trimethoxybenzene. ^c The slope of a linear Stern–Volmer plot at each concentration of Pr^nNH_2

Table 3. Photoamination of arenes with dimethyl- or diethyl-amine in the presence of DCNB

Arenes [mol dm ⁻³]	Amines [mol dm ⁻³]	Products, yield (%) ^b	Conversion of arene (%)	Recovery of DCNB (%)	φ^∞
(1) [0.05]	Me_2NH [0.2]	(15) 40 (21) 3 (24) 25	55	29	0.017
(1) [0.05]	Et_2NH [0.2]	(16) 26 (21) 6 (25) 2	31	49	0.004
(2) [0.05]	Me_2NH [0.2]	(17) 11 (24) 12	67	71	<0.005
(3) [0.05]	Me_2NH [0.2]	(18) 30 (24) 15	56	70	0.079
(4) [0.02]	Me_2NH [0.1]	(19) 76 (22) 11 (23) 4	96	98	0.32 ^c
(4) [0.05]	Et_2NH [0.05]	(20) 24 (22) 70 (23) 4	100	100	

^a $[\text{DCNB}]$ 0.1 mol dm⁻³ for the photoamination of (1)–(3), and 0.15 mol dm⁻³ for that of (4). ^b Isolated yields based on the arene used. Products: (23); 9,9',10,10'-tetrahydro-9,9'-bianthryl. ^c The limiting quantum yield for the disappearance of (4).

Table 4. Quenching of fluorescence of arenes by DCNB or amines^a

Arene	Quencher	$k_q\tau$ mol dm ⁻³	k_q mol dm ⁻³ s ⁻¹
(1)	DCNB	242	1.4×10^{10}
	RNH_2	<0.1	< 10^7
	Me_2NH	0.3	1.8×10^7
(2)	Et_2NH	0.8	4.7×10^7
	DCNB	1 320	1.3×10^{10}
(3)	Me_2NH	55	5.2×10^8
	DCNB	190	1.3×10^{10}
(4)	Me_2NH	3.7	2.5×10^8
	DCNB	75	1.4×10^{10}
	Me_2NH	1.5	2.8×10^8
	Et_2NH	3.5	6.6×10^8

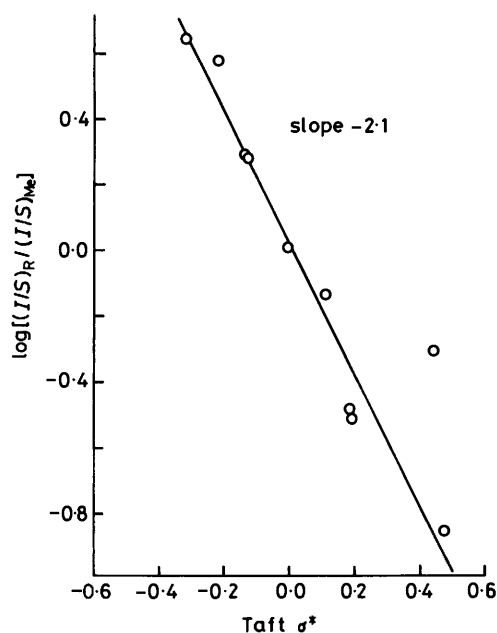
^a For argon-bubbled 9:1 acetonitrile–water solution of arenes $[1 \times 10^{-3} \text{ mol dm}^{-3}]$. ^b Calculated values using τ 17 ns for (1), 10.5 ns for (2), 15 ns for (3), and 5.3 ns for (4).¹⁵

of weak π -complexes of (1)⁺⁺ with RNH_2 can therefore be safely discarded. An alternative mechanism involving electron exchange between (1)⁺⁺ and RNH_2 is again unlikely to operate in the photoamination, since a plot of $\log(I/S)_R$ versus the ionization potential of RNH_2 is poorly correlated.

$$(\varphi^0)^{-1} = \frac{1}{\alpha\beta} \left(1 + \frac{k_X}{k_N[\text{RNH}_2]} + \frac{k_Q[\text{Q}]}{k_N[\text{RNH}_2]} \right) \quad (14)$$

$$K_{\text{SV}} = \frac{k_Q}{\alpha\beta k_N[\text{RNH}_2]} \quad (15)$$

Equation (14) represents the Stern–Volmer relationship for quenching of the photoamination by Q. Since the slope (K_{SV}) of

**Figure 4.** A plot of $\log[(I/S)_R/(I/S)_{\text{Me}}]$ versus Taft σ^* for the photoamination of (1) with RNH_2 in the presence of DCNB; data from Table 4

a Stern–Volmer plot of $(\varphi^0)^{-1}$ versus $[\text{Q}]$ at a given concentration of RNH_2 ($\text{R} = \text{Pr}^n$) can be written as equation (15), the slope of the plot of K_{SV} versus $[\text{RNH}_2]^{-1}$ in Figure 5 equals $k_Q/\alpha\beta k_N$.

Table 5. Taft σ^* and kinetic data

R	Taft σ^*	$\alpha\beta$	$(I/S)_R$	$\log(I/S)_R$	$\log \left[\frac{(I/S)_R}{(I/S)_{Me}} \right]$	$\frac{10^{-9}k_N}{\text{mol dm}^{-3} \text{ s}^{-1}}$
H	0.49	0.45	0.9	-0.03	-0.86	0.3
NCCH ₂ CH ₂	0.46	0.45	3.3	0.52	-0.31	1.0
HOCH ₂ CH ₂	0.20	0.36	1.9	0.29	-0.54	0.6
MeOCH ₂ CH ₂	0.19	0.42	2.2	0.34	-0.49	0.7
CH ₂ =CHCH ₂	0.13	0.14	5.0	0.70	-0.13	1.5
Me	0.00	0.20	6.7	0.83	0.00	2.0
Et	-0.10	0.15	13.0	1.11	0.28	4.0
Pr ⁿ	-0.115	0.16	13.2	1.12	0.29	4.0
Pr ⁱ	-0.19	0.16	25.8	1.41	0.58	7.9
Bu ⁱ	-0.30	0.14	29.2	1.47	0.64	8.9

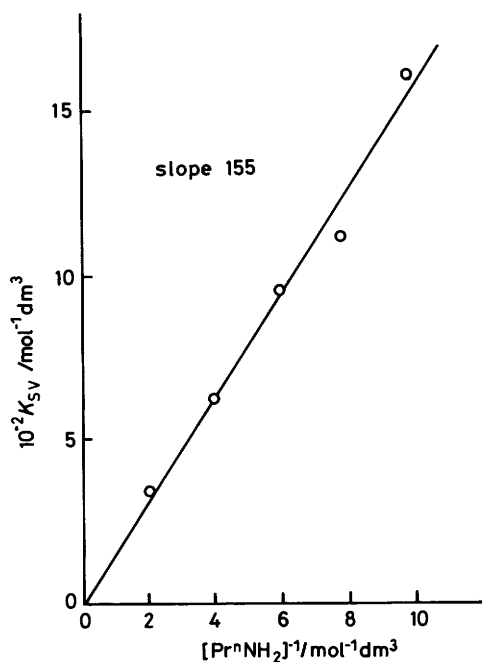


Figure 5. A plot of K_{SV} versus $[Pr^n NH_2]$ for quenching of the photoamination of (1) with $Pr^n NH_2$ by *p*-dimethoxybenzene; data from Table 2

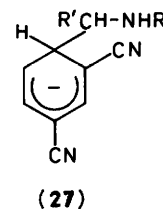
It is reasonable to assume that $k_Q \approx 10^{10} \text{ dm}^3 \text{ mol}^{-1} \text{ s}^{-1}$, since equation (9) is largely exothermic and since an essentially identical K_{SV} value was obtained in quenching of the photoamination by either *p*-di- or 1,3,5-tri-methoxybenzene even though the oxidation potentials of the quenchers are significantly different.¹⁰ On the basis of this assumption, k_N can be calculated to be $4.0 \times 10^8 \text{ dm}^3 \text{ mol}^{-1} \text{ s}^{-1}$ for $Pr^n NH_2$ since $\alpha\beta = 0.16$. For the other amines, therefore, the k_N values can be calculated from the ratios of $(I/S)_R$ to $(I/S)_{Pr^n}$, provided that the lifetime of $(1)^{+\cdot}$ ($1/k_X$) is constant, *ca.* 30 ns, independently of RNH_2 .

With regard to the rate constants, it should be noted that ArH cannot be hydroxylated nor methoxylated with H_2O or $MeOH$ upon irradiation of ArH in the presence of DCNB, an observation suggesting that k_N for H_2O or $MeOH$ should be much smaller than $10^6 \text{ dm}^3 \text{ mol}^{-1} \text{ s}^{-1}$. Presumably, either H_2O or $MeOH$ is too weak as a nucleophile to form a σ bond with $ArH^{+\cdot}$, even though weak π -complexes can be formed. On the other hand, $MeOH$ can add to the cation radical of 1,1-diphenylethylene¹¹ at $1.6 \times 10^9 \text{ dm}^3 \text{ mol}^{-1} \text{ s}^{-1}$, a consequence arising from much higher reactivities of this olefin cation radical compared with $ArH^{+\cdot}$. In other words, $ArH^{+\cdot}$ can react only

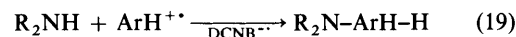
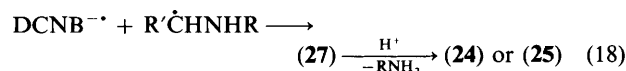
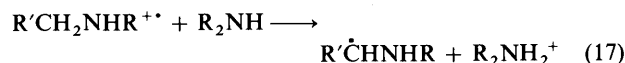
with such strong nucleophiles as CN^- ,² BH_4^- ,³ and RNH_2 ⁶ to give the corresponding addition products.

Mechanisms of Photoreactions of Arenes with R_2NH .— Although electron transfer from R_2NH to $^1ArH^*$ can occur in some cases,¹² the photoreactions of ArH with R_2NH were carried out under the conditions where the fluorescence of ArH is exclusively quenched by DCNB but negligibly by R_2NH . Therefore, equations (1)–(4) should again operate in the photoreactions with R_2NH . Nevertheless, the photoamination occurred only in poor yields with one exception unlike that with RNH_2 . Notable observations of mechanistic significance are (i) low quantum yields for the disappearance of ArH , (ii) considerable consumptions of DCNB, (iii) the formation of (24) and (25), and (iv) much lower oxidation potentials R_2NH compared with RNH_2 . It is of particular mechanistic interest to note that (4) can be efficiently photoaminated with Me_2NH but inefficiently with Et_2NH , an amine of lower oxidation potential than that of Me_2NH .

These observations strongly suggest that electron exchange



between $ArH^{+\cdot}$ and R_2NH , equation (16), can occur to regenerate ArH , thus resulting in the formation of (24) and (25) as the consequences of a radical-coupling reaction of $DCNB^{\cdot-}$ with an aminoalkyl radical formed by the loss of a proton from $R_2NH^{+\cdot}$, equations (17) and (18); this mechanism is very similar to that for the direct photoreaction of *p*-dicyanobenzene with triethylamine.¹³



Since R_2NH is a stronger nucleophile than RNH_2 ,¹⁴ the nucleophilic addition of R_2NH [equation (19)] can also occur competitively with equation (16) to give the aminated products in yields depending on relative importance of equations (16) and

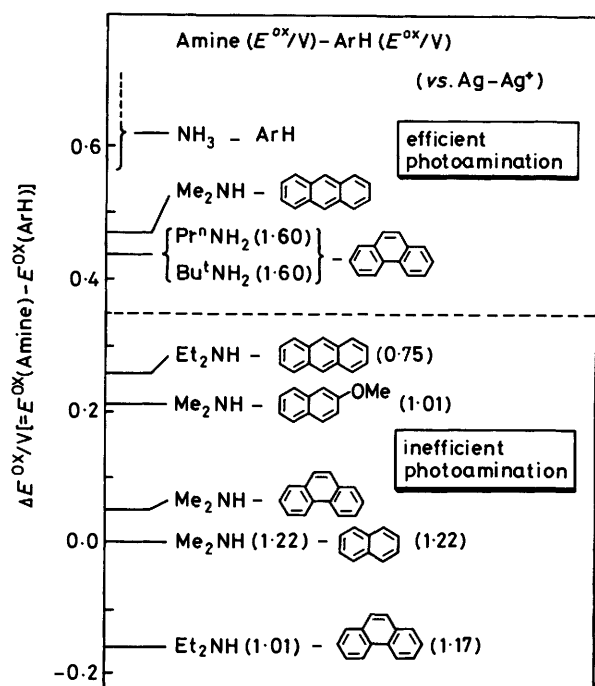
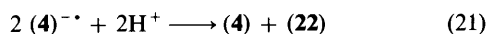


Figure 6. A schematic diagram for oxidation-potential differences between arenes and amines associated with efficiencies of the photoamination. A border lies at ΔE^{ox} ca. 0.3–0.4 eV

(19). The inefficient photoamination of (1)–(3) with R_2NH probably reflects the major occurrence of equation (16).

On the other hand, the efficient amination of (4) with Me_2NH is thus attributable to slower electron exchange compared with equation (19), since the oxidation potential of the amine is much more positive than that of (4). With Et_2NH , however, equation (16) should be again a major pathway, since the oxidation potential of this amine is similar to that of (4). It is of mechanistic interest to note that (22) is mainly formed in the photoreaction of (4) with Et_2NH , even though (4) $^{+\cdot}$ should be initially formed by equation (3). This can be attributed to the mechanistic sequence of electron transfer from $\text{DCNB}^{\cdot-}$ to (4) followed by disproportionation of (4) $^{\cdot-}$ in the presence of water, equations (20) and (21), since the reduction potential of (4) is similar to that of DCNB .¹⁵ This mechanism is also in accord with the quantitative recovery of DCNB as well as the lack of formation of (25). On the other hand, the reduction potentials of (1)–(3) are too negative for efficient electron transfer from $\text{DCNB}^{\cdot-}$ to occur. This is the reason for no or negligible formation of the corresponding reduced arenes accompanied by substantial consumption of DCNB .



Conclusions

The mechanism of the efficient photoamination of (1) with RNH_2 in the presence of DCNB has been established by kinetic analyses. A key mechanistic pathway is the nucleophilic addition of RNH_2 to the photogenerated cation radical of (1), the rate constant of which varies from $3 \times 10^7 \text{ dm}^3 \text{ mol}^{-1} \text{ s}^{-1}$ for NH_3 to $8.9 \times 10^8 \text{ dm}^3 \text{ mol}^{-1} \text{ s}^{-1}$ for Bu^tNH_2 . This mechanism should operate again in the efficient photoamination of the other arenes with RNH_2 . On the other hand, either Me_2NH or

Et_2NH undergoes electron exchange with the cation radical of (1)–(3) in competition with the nucleophilic addition, whereas the efficient addition of Me_2NH to (4) $^{+\cdot}$ can occur because of the low oxidation potential of (4). Figure 6 shows a diagram for differences between the observed oxidation potentials of the amines¹⁶ and ArH ,^{3,4} $\Delta E^{\text{ox}} = E^{\text{ox}}(\text{amine}) - E^{\text{ox}}(\text{ArH})$,* associated with observed features of the photoreactions. The efficient photoamination can occur in cases where $\Delta E^{\text{ox}} > 0.4$ eV. According to theoretical and empirical predictions on electron-transfer processes,¹⁷ the rate constant for electron transfer of 0.3–0.4 eV endothermicity is 10^6 – $10^7 \text{ dm}^3 \text{ mol}^{-1} \text{ s}^{-1}$, comparable with the rate constant for nucleophilic addition.

Experimental

¹H N.m.r., i.r., and u.v. spectra were, respectively, obtained on a JEOL JNM-60 spectrometer, a Hitachi 260-50 spectrometer, and a Hitachi 150-20 spectrometer. A Hitachi MPF-4 spectrofluorometer was used for fluorescence quenching experiments. Mass spectra were taken on a JEOL JMS-D300 equipped with a data analyser JMA-2000. Gas chromatography was performed on a Hitachi 163 or a Shimadzu GC-8A using a 50 cm column of 2% silicone OV-17 or 2% silicone OV-1 on Chromosorb W.

Spectral grade acetonitrile was distilled from P_2O_5 and then from CaH_2 . 2-Cyanoethylamine was prepared according to the literature method¹⁹ and purified by distillation. Aqueous solutions of ammonia, methylamine, and ethylamine were used without purification, while the other commercially available amines were distilled from KOH . All the arenes used were column chromatographed on silica gel and then recrystallized from ethanol. *m*-Dicyanobenzene was purified by recrystallization from methanol.

Preparative Photoamination of Phenanthrene with 2-Methoxyethylamine and n-Propylamine.—A 9:1 acetonitrile–water solution (140 cm^3) containing (1) (2.495 g, 14 mmol), DCNB (0.449 g, 3.5 mmol), and 2-methoxyethylamine (15.8 g, 210 mmol) or *n*-propylamine (12.4 g, 210 mmol) in a Pyrex vessel was irradiated with an Eikosha PIH-300 high-pressure mercury lamp for 13–20 h under cooling with water, as previously described.⁶ After evaporation under reduced pressure, the photolysates were dissolved in benzene (150 cm^3) and then extracted with dilute HCl . The acidic, aqueous layer was basified with saturated aqueous NaHCO_3 followed by extraction with Et_2O . Evaporation of the ether left the aminated product (8) [2.22 g, 93% yield based on (1) consumed] in the case of 2-methoxyethylamine or (12) (2.34 g, 95%) in the case of Pr^nNH_2 . The benzene layer was chromatographed on silica gel to recover 33% (1) and 77% DCNB in the case of 2-ethoxyethylamine or 26% (1) and 84% DCNB in the case of Pr^nNH_2 . Compound (8) had the following data: $\delta(\text{CCl}_4)$ 1.3 (br s, 1 H), 2.5–2.7 (m, 2 H), 2.9–3.0 (m, 2 H), 3.1 (s, 3 H), 3.2–3.5 (m, 2 H), 3.7 (t, J 5 Hz, 1 H), 6.9–7.3 (m, 6 H), and 7.4–7.6 (m, 2 H); m/z 253 (M^+); ν_{max} 3 310 cm^{-1} (N–H). The acetamide of (8) had m.p. 96–97 °C (from methanol) (Found: C, 76.9; H, 7.1; N, 4.6. $\text{C}_{19}\text{H}_{21}\text{NO}_2$ requires C, 77.3; H, 7.2; N, 4.7%). Compound (12) had the following data: $\delta(\text{CCl}_4)$ 0.8 (t, J 7 Hz, 3 H), 0.9 (br s, 1 H), 1.1–1.6 (m, 2 H), 2.3–2.5 (m, 2 H), 2.8–3.0 (m, 2 H), 3.6 (t, J 4.5 Hz, 1 H), 6.9–7.3 (m, 6 H), and 7.4–7.6 (m, 2 H); ν_{max} 3 310 cm^{-1} (N–H), m/z 237.

* The oxidation potential of dimethylamine was calculated from a linear correlation of the oxidation potentials [$E^{\text{ox}}(\text{amine})$ versus $\text{Ag}/\text{Ag}^+(\text{V})$]¹⁶ with the ionization potentials (IP)¹⁵ which was obtained for eight aliphatic amines; $E^{\text{ox}}(\text{amine}) = 0.806 \text{ IP} - 5.42$, an equation similar to that reported by Miller.¹⁸

Photoreactions of Naphthalene (2), 2-Methoxynaphthalene (3), and Anthracene (4) with Secondary Amines in the Presence of DCNB.—A 9:1 acetonitrile–water solution (140 cm³) containing (2) or (3) (7 mmol), DCNB (14 mmol), and Me₂NH (28 mmol) or a 19:1 acetonitrile–water solution (140 cm³) containing (4) (2.8 mmol), DCNB (21 mmol), and Et₂NH (7 mmol) was irradiated. The aminated products and the starting materials were isolated as described above. Irradiation time, yields of products, recovered yields of DCNB, and conversions of the arenes are listed in Table 3. The other photoreactions with R₂NH have been described elsewhere.⁶ Compound (17) had $\delta(\text{CCl}_4)$ 2.1 (s, 6 H), 3.1–3.3 (m, 2 H), 4.0–4.2 (m, 1 H), 5.7–5.9 (m, 2 H), and 6.7–7.0 (m, 4 H); m/z 173 (M^+), and 128 ($M - \text{HNMe}_2$). Compound (18) had $\delta(\text{CCl}_4)$ 1.9 and 2.1 (s, 6 H), 3.2–3.4 (m, 2 H), 3.45 and 3.5 (s, 3 H), 4.0 and 4.2 (t, J 3 Hz, 1 H), 4.85 (t, J 3 Hz, 1 H), and 6.9–7.0 (m, 4 H); m/z 203 (M^+), 158 ($M - \text{NHMe}_2$). Compound (20) had $\delta(\text{CCl}_4)$ 0.8 (t, J 6 Hz, 6 H), 2.4 (q, J 6 Hz, 4 H), 3.8 (ABq, J 18 Hz, 2 H), 4.5 (s, 1 H), and 6.8 (br s, 8 H).

Kinetic Experiments.—Aliquot portions (4 cm³) of reactant solutions and actinometer solutions were introduced into Pyrex tubes (8 mm, i.d.) and degassed by four freeze–pump–thaw cycles under high vacuum. Irradiation was carried out with a high-pressure mercury lamp under cooling with water by the use of appropriate light filters and a 'merry-go-round' turntable. A potassium chromate solution (0.2 g dm⁻³ in 0.1% NaOH aqueous solution, 10 mm path length) was used to isolate the 313 nm light whereas the 366 nm light was obtained by the passage through a Corning 7-37 glass filter and a solution of BiCl₃ (6.7 g dm⁻³ in 10% HCl aqueous solution, 10 mm path length). A hexan-2-one actinometer was used for the determination of quantum yields at 313 nm for the photoamination of (1)–(3), whereas those for the photoamination of (4) at 366 nm were determined with a potassium ferrioxalate actinometer. The formation of the aminated products (5)–(18) was quantitatively analysed by gas chromatography whereas the disappearance of (4) was followed by u.v. spectrometry.

Acknowledgements

We thank Professor Y. Tsuno, Kyushu University, for helpful discussions on substituent effects of aliphatic amines. This investigation was supported by Grant-in-Aid for Special Project Research from the Ministry of Education, Science, and Culture (Japan).

References

- 1 Part 43, M. Yasuda, T. Yamashita, K. Shima, and C. Pac, *J. Org. Chem.*, 1987, **52**, 753.
- 2 M. Yasuda, C. Pac, and H. Sakurai, *J. Chem. Soc., Perkin Trans. 1*, 1981, 746.
- 3 M. Yasuda, C. Pac, and H. Sakurai, *J. Org. Chem.*, 1981, **46**, 788.
- 4 T. Majima, C. Pac, A. Nakasone, and H. Sakurai, *J. Am. Chem. Soc.*, 1981, **103**, 4499.
- 5 M. Yasuda, C. Pac, and H. Sakurai, *Bull. Chem. Soc. Jpn.*, 1980, **53**, 502.
- 6 M. Yasuda, T. Yamashita, T. Matsumoto, K. Shima, and C. Pac, *J. Org. Chem.*, 1985, **50**, 3667.
- 7 J. F. Evans and H. N. Blount, *J. Am. Chem. Soc.*, 1978, **100**, 4191.
- 8 V. D. Parker, *Acc. Chem. Res.*, 1984, **17**, 243.
- 9 H. K. Hall, Jr., *J. Am. Chem. Soc.*, 1957, **79**, 5441; J. F. Coetzee and G. R. Padmanabhan, *ibid.*, 1965, **87**, 5006.
- 10 T. Majima, C. Pac, and H. Sakurai, *J. Am. Chem. Soc.*, 1980, **102**, 5265.
- 11 S. L. Mattes and S. Farid, *J. Am. Chem. Soc.*, 1986, **108**, 7356.
- 12 N. C. Yang and J. Libman, *J. Am. Chem. Soc.*, 1973, **95**, 5783.
- 13 M. Ohashi, K. Miyake, and K. Tsujimoto, *Bull. Chem. Soc. Jpn.*, 1980, **53**, 1683.
- 14 C. D. Ritchie and P. O. Virtanen, *J. Am. Chem. Soc.*, 1973, **95**, 1882.
- 15 S. L. Murov, 'Handbook of Photochemistry,' Marcel Dekker, New York, 1973.
- 16 C. K. Mann, *Anal. Chem.*, 1964, **36**, 2424; L. A. Hull, G. T. Davis, D. H. Rosenblatt, and C. K. Mann, *J. Phys. Chem.*, 1969, **73**, 2142.
- 17 R. A. Marcus, *J. Chem. Phys.*, 1956, **24**, 966; D. Rehm and A. Weller, *Isr. J. Chem.*, 1970, **8**, 259; F. Scandola and F. Balzani, *J. Am. Chem. Soc.*, 1979, **101**, 614.
- 18 L. L. Miller, G. D. Nordblom, and E. A. Mayeda, *J. Org. Chem.*, 1972, **37**, 916.
- 19 S. R. Buc, *Org. Synth.*, 1965, Coll. Vol. III, p. 93.

Received 18th May 1987; Paper 7/884